QCD sum rules for nucleons in nuclear matter III

Xuemin Jin, Marina Nielsen,* and Thomas D. Cohen
*Department of Physics and Center for Theoretical Physics, University of Maryland,
College Park, Maryland 20742*

R. J. Furnstahl
Department of Physics, The Ohio State University, Columbus, Ohio 43210

David K. Griegel†
Department of Physics and Nuclear Theory Center, Indiana University, Bloomington, Indiana 47405
(Received 19 July 1993)

The self-energies of quasinucleon states in nuclear matter are investigated using a finite-density QCD sum-rule approach developed previously. The sum rules are obtained for a general QCD interpolating field for the nucleon. The key phenomenological inputs are the nucleon σ term, the strangeness content of the nucleon, and quark and gluon distribution functions deduced from deep-inelastic scattering. The emphasis is on testing the sensitivity and stability of sum-rule predictions to variations of the condensates and other input parameters. At nuclear matter saturation density, the Lorentz vector self-energy is found to be positive with a magnitude of a few hundred MeV, which is comparable to that suggested by relativistic nuclear phenomenology. This result is quite stable. The prediction for the scalar self-energy is very sensitive to the undetermined values of the in-medium four-quark condensates.

I. INTRODUCTION

Connecting observed nuclear phenomena to the underlying theory of the strong interaction, quantum chromodynamics (QCD), is the ultimate goal of modern nuclear theory. This is difficult since most nuclear phenomena cannot be treated by perturbative methods. In the absence of a full solution to QCD at large distances, the QCD sum-rule method is a promising approach to making such connections. In a recent series of papers [1–4], QCD sum rules for nucleons in nuclear matter have been developed, with an emphasis on testing the predictions of relativistic nuclear phenomenology for quasinucleon self-energies. In this paper we extend this development.

The major goal of the QCD sum-rule approach in free space [5] is to extract the resonance properties of hadrons from perturbative QCD and the vacuum matrix elements of composite quark and gluon operators (condensates). The condensates parametrize nonperturbative features of the QCD vacuum and are independent of the hadrons considered. Applications of QCD sum-rule techniques over the past 15 years have had significant phenomenological success and have suggested that the spectral properties of many hadrons can be determined in terms of a small number of quark and gluon condensates [5–10].

*Permanent address: Instituto de Física, Universidade de São Paulo, 01498 SP Brazil.
†Present address: Department of Physics and Center for Theoretical Physics, University of Maryland, College Park, MD 20742.

Finite-density QCD sum rules for nucleons are based on the study of a correlation function of the nucleon interpolating field, which is constructed from quark fields and carries the quantum numbers of the nucleon. This correlator is evaluated in the ground state of infinite nuclear matter (rather than in the QCD vacuum). The nuclear matter ground state is characterized by ρ_N, the nucleon density in the rest frame, and u^μ, the four-velocity of the nuclear matter. For convenience, we choose to work in the rest frame of nuclear matter, where $u^\mu = (1, \mathbf{0})$. The analytic properties of the correlator as a function of the energy in this frame (with the three-momentum held fixed) can be made manifest by a Lehmann representation; the quasinucleon excitations are characterized by self-energies. By introducing a simple *Ansatz* for the spectral densities, one obtains a phenomenological representation of the correlation function.

On the other hand, the correlation function can be evaluated at large spacelike momenta using an operator product expansion (OPE). In this expansion of the correlator, matrix elements of composite quark and gluon operators in the nuclear matter ground state (in-medium condensates) are multiplied by coefficient functions (Wilson coefficients) evaluated using perturbative QCD. By equating the OPE and phenomenological representations and applying Borel transforms (see Sec. II), one obtains QCD sum rules that relate the nucleon self-energies to QCD Lagrangian parameters and finite-density condensates. Changes in the nucleon spectral properties at finite density are then related to changes in the condensates.

Isoscalar Lorentz scalar and vector self-energies that are large and canceling emerge naturally in a truncated

version of the finite-density nucleon sum rules [1,3], reflecting changes in the quark condensate $\langle \bar{q}q \rangle_{\rho_N}$ and the quark density $\langle q^\dagger q \rangle_{\rho_N}$. Such self-energies are consistent with those predicted by relativistic phenomenological models (e.g., Brueckner calculations [11,12] or the relativistic optical potentials of Dirac phenomenology [13,14]). In Refs. [3,4] these simple sum rules were extended by including the contributions of higher-energy states and higher-order terms in the OPE. The extended QCD sum-rule analysis indicates that the basic qualitative features of the simple sum rules might hold in the more complete analysis; whether or not this occurs depends on assumptions made about the density dependence of the four-quark condensates. In this paper we derive the finite-density nucleon sum rules with a more general nucleon interpolating field and present further details of the sum-rule analysis. We include a variety of corrections outlined in Refs. [3,4] and study the sensitivity of our results to various parameters in the sum rules.

At finite density, the ground state is not Lorentz invariant; therefore, expectation values of local operators with any integer spin can be nonzero in nuclear matter [4]. As a result, a large number of new terms (i.e., terms that vanish in the vacuum) appear in the OPE at finite density; terms present in the OPE in vacuum also become density dependent. We construct the OPE so that all density dependence of the correlator resides in the condensates. We estimate these condensates to first order in the nucleon density ρ_N. We assume that applying this approximation up to nuclear matter saturation density is reasonable for calculating scalar and vector self-energies. Then the in-medium condensates can be written as $\langle \hat{O} \rangle_{\rho_N} = \langle \hat{O} \rangle_{\text{vac}} + \langle \hat{O} \rangle_N \rho_N$, where $\langle \hat{O} \rangle_{\rho_N}$ is the in-medium condensate, $\langle \hat{O} \rangle_{\text{vac}}$ is the vacuum condensate, and $\langle \hat{O} \rangle_N$ is the expectation value of the operator in a nucleon state (at rest) [4]. In this paper we consider the contributions from quark and quark-gluon condensates up to dimension five, from dimension-four gluon condensates, and from dimension-six four-quark condensates. Perturbative corrections to the operators are taken into account in the leading-logarithmic approximation through anomalous-dimension factors [5].

In nuclear matter, nucleon and antinucleon spectral properties are not simply related by discrete symmetries, since the ground state is no longer invariant under charge conjugation. Our assumptions about the finite-density phenomenological spectral functions are motivated from basic features of observed nuclear phenomena. In particular, the positive-energy nucleon pole becomes a broadened peak in the medium, which reflects the spreading of strength into other states. Nevertheless, the comparatively small imaginary parts of the optical potentials suggested by Dirac phenomenology and meson-exchange models indicate that the peak remains narrow on hadronic energy scales [11–14]. Since the sum rule averages over the spectral function on such scales, a pole Ansatz for the quasinucleon is justified. A Lorentz covariant quasinucleon pole Ansatz automatically includes a negative-energy nucleon pole, which corresponds to an antinucleon propagating in nuclear matter. However, we

have much less information about the negative-energy nucleon pole and we expect that, in nature, the antinucleon pole is broadened significantly due to annihilation processes. Our calculational strategy is to construct the sum rules so as to suppress contributions from the vicinity of the negative-energy pole [3]. Contributions from higher-energy continuum states are included using a rough approximation, which starts at an effective continuum threshold.

We find that the finite-density QCD sum rules predict a large and positive (i.e., repulsive) Lorentz vector self-energy for a nucleon in nuclear matter. This self-energy is essentially proportional to the nucleon density. The predicted ratio of the vector self-energy to the zero-density nucleon mass is found to be relatively insensitive to the details of the calculations and quite stable against variations of the condensates and parameters. In contrast, the prediction for the Lorentz scalar self-energy is very sensitive to the assumed density dependence of the four-quark condensates and to the value of the nucleon σ term. We find that the ratio of the scalar self-energy to the free-space nucleon mass is insensitive to the Borel mass M when the density dependence of these condensates is weak or moderate and is sensitive to the Borel mass M when these condensates have a strong density dependence (see Secs. II and III). If we assume that the four-quark condensates have a weak density dependence, then we find that sum rules predict a large and negative scalar self-energy that cancels the vector self-energy. This result is in good agreement with relativistic phenomenology. A basic disagreement with the known empirical situation is found when the four-quark condensates depend strongly on the nucleon density.

There have been several other recent papers that focus on similar or related topics. Drukarev and Levin [15] have studied QCD sum rules for nucleons in nuclear matter using an OPE and dispersion relations that differ from those considered here and in Refs. [3,4]. They have focused on the properties of nuclear matter, such as the saturation curve. We note that QCD sum-rule predictions for nuclear matter saturation properties require detailed knowledge of the density dependence of the condensates, particularly the in-medium quark condensate $\langle \bar{q}q \rangle_{\rho_N}$ and the in-medium four-quark condensates. It is not obvious that our present knowledge of this density dependence is precise enough to allow a meaningful description of saturation. In Ref. [16] Henley and Pasupathy use a somewhat different formalism; their approach is based on nucleon-nucleus scattering as opposed to the propagation of a nucleon in nuclear matter. In Refs. [17,18] nucleon sum rules were used to estimate the density dependence of the neutron-proton mass difference, which might account for the Nolen-Schiffer anomaly. Sum rules for vector mesons in nuclear matter were discussed in Refs. [19,20].

The rest of this paper is organized as follows. In Sec. II we derive QCD sum rules for nucleons in nuclear matter with a general interpolating field. In Sec. III typical numerical results are presented. A detailed analysis of the sensitivity to various inputs is given in Sec. IV; additional discussion is given in Sec. V.

II. SUM RULES FOR THE NUCLEON IN NUCLEAR MATTER

In this section we derive QCD sum rules for nucleons in infinite nuclear matter with a general interpolating field, following the method developed in Refs. [1,3,4]. In the operator product expansion (OPE) for the nucleon correlator, we work to leading order in perturbation theory; leading-logarithmic corrections to the sum rules are included through anomalous-dimension factors. Contributions proportional to the up and down current quark masses are neglected as they give numerically small contributions. We consider quark and quark-gluon condensates up to dimension five and pure gluon condensates of dimension four. At dimension six we include only the four-quark condensates; all other dimension-six and higher-dimensional condensates are neglected since we expect their contributions to be small in the region of optimal Borel mass [4]. If the sum rules are correct, the inclusion of such contributions should make the "window" in the Borel mass larger and the "plateaus" in the predicted quantities as functions of the Borel mass flatter.

As discussed earlier in Refs. [1,3,4], QCD sum rules for the nucleon at finite density focus on the nucleon correlator defined by

$$\Pi(q) \equiv i \int d^4x \, e^{iq \cdot x} \langle \Psi_0 | T[\eta(x)\bar{\eta}(0)] | \Psi_0 \rangle \ , \qquad (2.1)$$

where $\eta(x)$ is a colorless interpolating field made up of quark fields that has the quantum numbers of a nucleon. The ground state of nuclear matter $|\Psi_0\rangle$ is characterized by the rest-frame nucleon density ρ_N and by the four-velocity u^μ; it is assumed to be invariant under parity and time reversal except for the transformation of u^μ.

We consider nucleon interpolating fields (currents) that contain no derivatives and couple to spin-$\frac{1}{2}$ states only. There are two linearly independent fields with these features, corresponding to a scalar or pseudoscalar diquark coupled to a quark. For the proton these two independent interpolating fields are

$$\eta_1(x) = \epsilon_{abc}[u_a^T(x)C\gamma_5 d_b(x)]u_c(x) \ , \qquad (2.2)$$

$$\eta_2(x) = \epsilon_{abc}[u_a^T(x)C d_b(x)]\gamma_5 u_c(x) \ , \qquad (2.3)$$

where T denotes a transpose in Dirac space and C is the charge conjugation matrix. The analogous fields for the neutron follow by interchanging the up and down quark fields.

In this paper we take a linear combination of these two fields,

$$\eta(x) = 2[t\eta_1(x) + \eta_2(x)] \ , \qquad (2.4)$$

where t is an arbitrary real parameter. The interpolating field with $t = -1$, advocated by Ioffe [6], corresponds to an axial vector diquark coupled to a quark. This interpolating field has been used exclusively in previous papers on finite-density nucleon sum rules [1,3,4]. In principle, the sum-rule predictions are independent of the choice of t; in practice, however, the OPE is truncated and

the phenomenological description is represented roughly. The goals in choosing the interpolating field for QCD sum-rule applications are to maximize the coupling of the interpolating field to the state of interest relative to other (continuum) states, while minimizing the contributions of higher-order terms in the OPE. These goals cannot be simultaneously realized. The optimal choice of the nucleon interpolating field seems to be close to Ioffe's choice. We refer the reader to Ref. [21] for more discussion about Ioffe's interpolating field. Interpolating fields with t around -1.1 have also been used in nucleon sum-rule studies [22], particularly in studying direct small-scale instanton effects in the nucleon sum rules [23,24]. To reflect this range of t, we shall consider the interval $-1.15 \leq t \leq -0.95$ here. For $t > -0.95$ the continuum contributions become large while for $t < -1.15$ the contributions from higher-order terms in the OPE become important relative to the leading-order terms.

Lorentz covariance, parity, and time reversal allow one to decompose the correlator into three distinct structures [1,3,4]:

$$\Pi(q) \equiv \Pi_s(q^2, q \cdot u) + \Pi_q(q^2, q \cdot u)\slashed{q} + \Pi_u(q^2, q \cdot u)\slashed{u} \ . \quad (2.5)$$

The three invariant functions, Π_s, Π_q, and Π_u, can be projected out by taking appropriate traces of $\Pi(q)$ [3,4]. In vacuum, Π_s and Π_q become functions of q^2 only and Π_u vanishes. For convenience, we will work in the rest frame of nuclear matter hereafter, which implies $u^\mu \to (1, \mathbf{0})$; we also take $\Pi_i(q^2, q \cdot u) \to \Pi_i(q_0, |\mathbf{q}|)$ ($i = \{s, q, u\}$). To obtain sum rules, we construct a phenomenological representation for $\Pi(q)$ using a simple spectral *Ansatz* and evaluate $\Pi(q)$ at large spacelike q^2 using the OPE.

The analytic properties of $\Pi(q)$ can be studied through a Lehmann representation, in which all of the singularities of $\Pi(q)$ in q_0 lie on the real q_0 axis. For each of the Lorentz structures Π_i we can write a dispersion relation of the form [3]

$$\Pi_i(q_0, |\mathbf{q}|) = \frac{1}{2\pi i} \int_{-\infty}^{\infty} d\omega \, \frac{\Delta\Pi_i(\omega, |\mathbf{q}|)}{\omega - q_0} \ , \qquad (2.6)$$

where we have omitted polynomials arising from the contour at infinity [25], which will be eliminated by a subsequent Borel transform. We have also omitted infinitesimals, which determine for real q_0 whether the correlator is retarded, advanced, or time ordered; they are not needed since the present formulation of the QCD sum rules only applies Eq. (2.6) with q_0 off the real axis [3]. The discontinuity, defined by

$$\Delta\Pi_i(\omega, |\mathbf{q}|) \equiv \lim_{\epsilon \to 0^+} [\Pi_i(\omega + i\epsilon, |\mathbf{q}|) - \Pi_i(\omega - i\epsilon, |\mathbf{q}|)] \ , \qquad (2.7)$$

contains the spectral information on the quasiparticle, quasihole, and higher-energy states.

In QCD sum-rule applications, one parametrizes the spectral density with a small number of spectral parameters characterizing the resonances in the channel of interest (e.g., poles, residues, etc.). At finite density, the

ground state is no longer invariant under charge conjugation; thus the spectral densities for baryons and antibaryons are not simply related. For the nucleon, the characteristics of the phenomenological Dirac optical potentials for intermediate-energy proton-nucleus scattering and those obtained from meson-exchange models suggest that a nucleon in nuclear matter can be regarded as a quasiparticle with large scalar and vector self-energies. The imaginary parts of the optical potentials suggest that the width of the quasinucleon excitation is relatively small on hadronic scales; thus a pole approximation for the positive-energy quasinucleon should be justified. In contrast, an antinucleon propagating in nuclear matter is expected to be much broader due to annihilation processes. The reader is referred to Ref. [3] for more motivation for using the QCD sum-rule approach and for using a quasinucleon pole approximation.

We assume a quasiparticle pole for the nucleon, so that the self-energies are real and depend only on $|\mathbf{q}|$; all higher-energy excitations are included in a continuum contribution. Lorentz covariance then dictates the representations of the individual invariant functions [3]:

$$\Pi_s(q_0, |\mathbf{q}|) = -\lambda_N^{*2} \frac{M_N^*}{(q_0 - E_q)(q_0 - \overline{E}_q)} + \cdots , \qquad (2.8)$$

$$\Pi_q(q_0, |\mathbf{q}|) = -\lambda_N^{*2} \frac{1}{(q_0 - E_q)(q_0 - \overline{E}_q)} + \cdots , \qquad (2.9)$$

$$\Pi_u(q_0, |\mathbf{q}|) = +\lambda_N^{*2} \frac{\Sigma_v}{(q_0 - E_q)(q_0 - \overline{E}_q)} + \cdots , \qquad (2.10)$$

where λ_N^* is the residue at the quasinucleon pole, which specifies the coupling of the interpolating field to the physical quasinucleon state, and the ellipses denote the contributions from higher-energy states, which will be included later. Here we have defined

$$M_N^* \equiv M_N + \Sigma_s , \qquad (2.11)$$

$$E_q \equiv \Sigma_v + \sqrt{\mathbf{q}^2 + M_N^{*2}} , \qquad (2.12)$$

$$\overline{E}_q \equiv \Sigma_v - \sqrt{\mathbf{q}^2 + M_N^{*2}} , \qquad (2.13)$$

where Σ_s and Σ_v are the scalar and vector self-energies

of the nucleon in nuclear matter, respectively [3].

The quasinucleon (positive-energy) pole is at E_q. We observe that a negative-energy pole, occurring at $\overline{E}_q$, is introduced in Eqs. (2.8)–(2.10). This corresponds to an antinucleon quasiparticle added to the nuclear matter. Since the narrow-resonance approximation for an antinucleon is not justified and since we wish to focus only on the positive-energy quasinucleon pole, we construct sum rules that suppress the contributions from the region of the negative-energy excitations.

We proceed now to evaluate $\Pi(q)$ at short distances, i.e., $q^2 \to -\infty$, using the OPE [26,27]. In the present approach, we use a dispersion relation in q_0 with the three-momentum held fixed to specify the quasinucleon state to be studied [see Eq. (2.6)]; therefore, we need to apply the OPE in the limit that q_0 becomes large and imaginary while $|\mathbf{q}|$ remains fixed (in the nuclear matter rest frame). This limit takes $q^2 \to -\infty$ with $|q^2/q_0| \to \infty$, which satisfies the conditions discussed in Ref. [27] for a short-distance expansion.

Applying the OPE to the time-ordered product in Eq. (2.1), one can express the invariant functions of the nucleon correlator in the form [4,3]

$$\Pi_i(q^2, q_0) = \sum_n C_n^i(q^2, q_0)\langle \widehat{O}_n \rangle_{\rho_N} , \qquad (2.14)$$

where $\langle \widehat{O}_n \rangle_{\rho_N} \equiv \langle \Psi_0 | \widehat{O}_n | \Psi_0 \rangle$. The Wilson coefficients $C_n^i(q^2, q_0)$ depend only on QCD Lagrangian parameters; all of the density dependence of the correlator is included in the matrix elements $\langle \widehat{O}_n \rangle_{\rho_N}$ (the in-medium condensates).[1]

The calculation of the Wilson coefficients in the OPE is straightforward using the simple rules and techniques outlined in Ref. [4]. For convenience we separate the invariant functions into pieces that are even and odd in q_0:

$$\Pi_i(q_0, |\mathbf{q}|) = \Pi_i^E(q_0^2, |\mathbf{q}|) + q_0 \Pi_i^O(q_0^2, |\mathbf{q}|) . \qquad (2.15)$$

Working to leading order in perturbation theory and using the general nucleon interpolating field [Eq. (2.4)], we obtain

$$\Pi_s^E = \frac{c_1}{16\pi^2} q^2 \ln(-q^2)\langle \overline{q}q \rangle_{\rho_N} + \frac{3c_2}{16\pi^2} \ln(-q^2)\langle g_s \overline{q}\sigma \cdot \mathcal{G}q \rangle_{\rho_N} + \frac{2c_3}{3\pi^2} \frac{q_0^2}{q^2}(\langle \overline{q}iD_0 iD_0 q \rangle_{\rho_N} + \tfrac{1}{8}\langle g_s \overline{q}\sigma \cdot \mathcal{G}q \rangle_{\rho_N}) , \qquad (2.16)$$

$$\Pi_s^O = -\frac{c_1}{8\pi^2} \ln(-q^2)\langle \overline{q}iD_0 q \rangle_{\rho_N} - \frac{c_1}{3q^2} \langle \overline{q}q \rangle_{\rho_N} \langle q^\dagger q \rangle_{\rho_N} , \qquad (2.17)$$

$$\Pi_q^E = -\frac{c_4}{512\pi^4}(q^2)^2 \ln(-q^2) + \frac{c_4}{72\pi^2}\left(5\ln(-q^2) - \frac{8q_0^2}{q^2}\right)\langle q^\dagger iD_0 q \rangle_{\rho_N} + \frac{c_4}{128\pi^2} \ln(-q^2)\left\langle \frac{\alpha_s}{\pi}(\mathbf{E}^2 - \mathbf{B}^2)\right\rangle_{\rho_N}$$
$$+ \frac{c_4}{1152\pi^2}\left(\ln(-q^2) - \frac{4q_0^2}{q^2}\right)\left\langle \frac{\alpha_s}{\pi}(\mathbf{E}^2 + \mathbf{B}^2)\right\rangle_{\rho_N} - \frac{c_1}{6q^2}\langle \overline{q}q \rangle_{\rho_N}^2 - \frac{c_4}{6q^2}\langle q^\dagger q \rangle_{\rho_N}^2 , \qquad (2.18)$$

$$\Pi_q^O = \frac{c_4}{24\pi^2} \ln(-q^2)\langle q^\dagger q \rangle_{\rho_N} + \frac{c_5}{72\pi^2 q^2}\langle g_s q^\dagger \sigma \cdot \mathcal{G}q \rangle_{\rho_N} - \frac{c_4}{12\pi^2 q^2}\left(1 + \frac{2q_0^2}{q^2}\right)(\langle q^\dagger iD_0 iD_0 q \rangle_{\rho_N} + \tfrac{1}{12}\langle g_s q^\dagger \sigma \cdot \mathcal{G}q \rangle_{\rho_N}) , \qquad (2.19)$$

---

[1]The dependence of $C_n^i(q^2, q_0)$ and $\langle \widehat{O}_n \rangle_{\rho_N}$ on the normalization point μ has been suppressed [28,29].

$$\Pi_u^E = \frac{c_4}{12\pi^2}q^2\ln(-q^2)\langle q^\dagger q\rangle_{\rho_N} - \frac{c_5}{48\pi^2}\ln(-q^2)\langle g_s q^\dagger\sigma\cdot\mathcal{G}q\rangle_{\rho_N} + \frac{c_4}{2\pi^2}\frac{q_0^2}{q^2}(\langle q^\dagger iD_0 iD_0 q\rangle_{\rho_N} + \tfrac{1}{12}\langle g_s q^\dagger\sigma\cdot\mathcal{G}q\rangle_{\rho_N})\ , \tag{2.20}$$

$$\Pi_u^O = -\frac{5c_4}{18\pi^2}\ln(-q^2)\langle q^\dagger iD_0 q\rangle_{\rho_N} - \frac{c_4}{288\pi^2}\ln(-q^2)\left\langle\frac{\alpha_s}{\pi}(\mathbf{E}^2+\mathbf{B}^2)\right\rangle_{\rho_N} - \frac{c_4}{3q^2}\langle q^\dagger q\rangle_{\rho_N}^2\ , \tag{2.21}$$

where all polynomials in q^2 and q_0^2, which vanish under the Borel transform, have been omitted. Here we have adopted the notation of Ref. [4] and have defined

$$c_1 = 7t^2 - 2t - 5\ , \tag{2.22}$$
$$c_2 = 1 - t^2\ , \tag{2.23}$$
$$c_3 = 2t^2 - t - 1\ , \tag{2.24}$$
$$c_4 = 5t^2 + 2t + 5\ , \tag{2.25}$$
$$c_5 = 7t^2 + 10t + 7\ . \tag{2.26}$$

Contributions from four-quark condensates are included in factorized form [4]. (See Sec. III for discussion of the factorization approximation.)

QCD sum rules for the nucleon follow by comparing the phenomenological representation to the OPE representation. In vacuum sum rules, the overlap of the two descriptions is improved by applying a Borel transform. Here we use a finite-density generalization of the vacuum sum rules that improves the overlap of the two descriptions, suppresses contributions from negative-energy excitations, and reduces to the vacuum sum rules in the zero-density limit (see Ref. [3] for a detailed discussion). Sum rules for the nucleon are constructed as

$$\mathcal{B}[\Pi_i^E(q_0^2,|\mathbf{q}|) - \overline{E}_q\Pi_i^O(q_0^2,|\mathbf{q}|)]_{\mathrm{OPE}}$$
$$= \mathcal{B}[\Pi_i^E(q_0^2,|\mathbf{q}|) - \overline{E}_q\Pi_i^O(q_0^2,|\mathbf{q}|)]_{\mathrm{phen}}\ , \tag{2.27}$$

for $i = \{s, q, u\}$, where the left-hand side is obtained from the OPE, the right-hand side is obtained from the dispersion relations using a simple phenomenological spectral Ansatz, and $\mathcal{B}$ is the Borel transform operator defined by

$$\mathcal{B}[f(q_0^2,|\mathbf{q}|)] \equiv \lim_{\substack{-q_0^2,n\to\infty \\ -q_0^2/n=M^2}} \frac{(-q_0^2)^{n+1}}{n!}\left(\frac{\partial}{\partial q_0^2}\right)^n f(q_0^2,|\mathbf{q}|)$$
$$\equiv \hat{f}(M^2,|\mathbf{q}|)\ , \tag{2.28}$$

where M is known as the Borel mass. In Eq. (2.27), $\overline{E}_q$ is the energy of the negative-energy pole in the quasiparticle Ansatz [see Eqs. (2.8)–(2.10)]. Sum rules constructed in this manner completely suppress sharp excitations at $\overline{E}_q$ and also strongly suppress a broad excitation in this vicinity.

Perturbative corrections $\sim \alpha_s^n$ can be taken into ac-

count in the leading-logarithmic approximation through anomalous-dimension factors [5]. After the Borel transform, the effect of these corrections is to multiply each term on the OPE side of the sum rules by the factor [6–8]

$$L^{-2\Gamma_\eta + \Gamma_{O_n}} \equiv \left[\frac{\ln(M/\Lambda_{\mathrm{QCD}})}{\ln(\mu/\Lambda_{\mathrm{QCD}})}\right]^{-2\Gamma_\eta + \Gamma_{O_n}}\ , \tag{2.29}$$

where Γ_η is the anomalous dimension of the interpolating field η, Γ_{O_n} is the anomalous dimension of the corresponding local operator, μ is the normalization point of the operator product expansion, and Λ_{QCD} is the QCD scale parameter. We take $\mu = 0.5\,\mathrm{GeV}$ and $\Lambda_{\mathrm{QCD}} = 100\,\mathrm{MeV}$ [8] in our calculations. The anomalous dimensions Γ_η and Γ_{O_n} depend on N_f, the number of flavors.[2] We take $N_f = 3$ in this paper, as the effect of heavy virtual quarks turns out to be negligible [5]. For the interpolating field defined in Eq. (2.4), we have $\Gamma_\eta = \tfrac{2}{9}$ [30]. The anomalous dimension of $\overline{q}q$ is $\tfrac{4}{9}$ [5]. Since $\overline{q}\gamma^\mu q$ is a conserved current, the anomalous dimension for this operator is 0.

For dimension-four and -five operators we will adopt the values of the corresponding condensates at the scale of 1 GeV and ignore the anomalous dimensions of these operators (i.e., set $\Gamma_{O_n} = 0$), either because the operators are renormalization-group invariant (so that $\Gamma_{O_n} = 0$), because the anomalous dimension is small, because the corresponding condensates give small contributions, or because the accuracy to which the nucleon matrix elements of the operators are known is such that anomalous-dimension corrections represent an unwarrantable refinement.

The four-quark operators are not, in general, renormalization covariant, so they mix with one another under the renormalization group [5]. In vacuum, the anomalous-dimension effects do not violate the factorization assumption to within 10% [5], and thus one assumes that the anomalous dimension of a four-quark operator is equal to the sum of the anomalous dimensions of the factorized operators [6,7]. In this paper we follow this assumption.

With the spectral Ansätze of Eqs. (2.8)–(2.10) and the OPE results of Eqs. (2.16)–(2.21), we obtain three sum rules—one for each invariant function:

$$\lambda_N^{*2}M_N^* e^{-(E_q^2-\mathbf{q}^2)/M^2} = -\frac{c_1}{16\pi^2}M^4 E_1\langle\overline{q}q\rangle_{\rho_N} - \frac{c_1}{8\pi^2}\overline{E}_q M^2 E_0\langle\overline{q}iD_0 q\rangle_{\rho_N}L^{-4/9} - \frac{3c_2}{16\pi^2}M^2 E_0\langle g_s\overline{q}\sigma\cdot\mathcal{G}q\rangle_{\rho_N}L^{-4/9}$$
$$-\frac{2c_3}{3\pi^2}\mathbf{q}^2(\langle\overline{q}iD_0 iD_0 q\rangle_{\rho_N} + \tfrac{1}{8}\langle g_s\overline{q}\sigma\cdot\mathcal{G}q\rangle_{\rho_N})L^{-4/9} - \frac{c_1}{3}\overline{E}_q\langle\overline{q}q\rangle_{\rho_N}\langle q^\dagger q\rangle_{\rho_N}\ , \tag{2.30}$$

[2]The factor $1/b$ $(b = 11 - \tfrac{2}{3}N_f)$ is included in the definition of Γ_η and Γ_{O_n} (see Refs. [6,7,30]).

$$\lambda_N^{*2} e^{-(E_q^2-\mathbf{q}^2)/M^2} = \frac{c_4}{256\pi^4}M^6 E_2 L^{-4/9} + \frac{c_4}{24\pi^2}\overline{E}_q M^2 E_0\langle q^\dagger q\rangle_{\rho_N} L^{-4/9} - \frac{c_4}{72\pi^2}M^2\left(5E_0 - \frac{8\mathbf{q}^2}{M^2}\right)\langle q^\dagger iD_0 q\rangle_{\rho_N} L^{-4/9}$$

$$- \frac{c_4}{128\pi^2}M^2 E_0\left\langle\frac{\alpha_s}{\pi}(\mathbf{E}^2-\mathbf{B}^2)\right\rangle_{\rho_N} L^{-4/9} - \frac{c_4}{1152\pi^2}M^2\left(E_0 - \frac{4\mathbf{q}^2}{M^2}\right)\left\langle\frac{\alpha_s}{\pi}(\mathbf{E}^2+\mathbf{B}^2)\right\rangle_{\rho_N} L^{-4/9}$$

$$+ \frac{c_5}{72\pi^2}\overline{E}_q\langle g_s q^\dagger\sigma\cdot\mathcal{G}q\rangle_{\rho_N} L^{-4/9} - \frac{c_4}{12\pi^2}\overline{E}_q\left(3 - \frac{2\mathbf{q}^2}{M^2}\right)(\langle q^\dagger iD_0 iD_0 q\rangle_{\rho_N} + \tfrac{1}{12}\langle g_s q^\dagger\sigma\cdot\mathcal{G}q\rangle_{\rho_N})L^{-4/9}$$

$$+ \frac{c_1}{6}\langle\bar{q}q\rangle_{\rho_N}^2 L^{4/9} + \frac{c_4}{6}\langle q^\dagger q\rangle_{\rho_N}^2 L^{-4/9} , \tag{2.31}$$

$$\lambda_N^{*2}\Sigma_v e^{-(E_q^2-\mathbf{q}^2)/M^2} = \frac{c_4}{12\pi^2}M^4 E_1\langle q^\dagger q\rangle_{\rho_N} L^{-4/9} + \frac{5c_4}{18\pi^2}\overline{E}_q M^2 E_0\langle q^\dagger iD_0 q\rangle_{\rho_N} L^{-4/9}$$

$$+ \frac{c_4}{288\pi^2}\overline{E}_q M^2 E_0\left\langle\frac{\alpha_s}{\pi}(\mathbf{E}^2+\mathbf{B}^2)\right\rangle_{\rho_N} L^{-4/9} - \frac{c_5}{48\pi^2}M^2 E_0\langle g_s q^\dagger\sigma\cdot\mathcal{G}q\rangle_{\rho_N} L^{-4/9}$$

$$+ \frac{c_4}{2\pi^2}\mathbf{q}^2(\langle q^\dagger iD_0 iD_0 q\rangle_{\rho_N} + \tfrac{1}{12}\langle g_s q^\dagger\sigma\cdot\mathcal{G}q\rangle_{\rho_N})L^{-4/9} + \frac{c_4}{3}\overline{E}_q\langle q^\dagger q\rangle_{\rho_N}^2 L^{-4/9} . \tag{2.32}$$

Here we have defined the following quantities, which account for continuum corrections to the sum rules [3]:

$$E_0 \equiv 1 - e^{-s_0^*/M^2} , \tag{2.33}$$

$$E_1 \equiv 1 - e^{-s_0^*/M^2}\left(\frac{s_0^*}{M^2} + 1\right) , \tag{2.34}$$

$$E_2 \equiv 1 - e^{-s_0^*/M^2}\left(\frac{s_0^{*2}}{2M^4} + \frac{s_0^*}{M^2} + 1\right) , \tag{2.35}$$

where we define the continuum threshold $s_0^* \equiv \omega_0^2 - \mathbf{q}^2$ (ω_0 is the energy at the continuum threshold). In principle, the effective thresholds are different for positive and negative energies and for the different sum rules. The former differences are critical in some sum-rule formulations [31], but are not numerically important in the present formulation. Furthermore, the thresholds are relatively poorly determined by the sum rules and effects due to different thresholds in different sum rules may be absorbed by slight changes in the other parameters. In this paper we use a universal effective threshold for simplicity.

III. RESULTS

A. In-medium condensates

To extract the self-energies from the finite-density nucleon sum rules, one has to know the in-medium condensates appearing in the sum rules. Working to leading order in the nucleon density ρ_N, one can write

$$\langle\hat{O}\rangle_{\rho_N} = \langle\hat{O}\rangle_{\text{vac}} + \langle\hat{O}\rangle_N\rho_N + \cdots , \tag{3.1}$$

where the ellipsis denotes correction terms that are of higher order in ρ_N, and $\langle\hat{O}\rangle_N$ is the spin-averaged nucleon matrix element. Note that this is not a Taylor expansion in ρ_N. For a general operator $\hat{O}$ there is not a systematic way to study contributions to $\langle\hat{O}\rangle_{\rho_N}$ that are of higher order in ρ_N. Model-dependent estimates in Ref. [2] suggest that the linear approximation to

$\langle\bar{q}q\rangle_{\rho_N}$ should be good (higher-order corrections $\sim 20\%$ of the linear term) up to nuclear matter saturation density. Here we assume the first-order approximation of all condensates to be reasonable for calculating scalar and vector self-energies up to nuclear matter saturation density. Verifying the limits of this type of density expansion is an important problem for future study.

The most important condensates in the finite-density nucleon sum rules are the dimension-three quark condensates $\langle\bar{q}q\rangle_{\rho_N}$ and $\langle q^\dagger q\rangle_{\rho_N}$. The former condensate has been evaluated and discussed in detail in Refs. [2,15]; the latter condensate is simply proportional to the nucleon density:

$$\langle\bar{q}q\rangle_{\rho_N} = \langle\bar{q}q\rangle_{\text{vac}} + \frac{\sigma_N}{2m_q}\rho_N , \tag{3.2}$$

$$\langle q^\dagger q\rangle_{\rho_N} = \tfrac{3}{2}\rho_N , \tag{3.3}$$

where $m_q \equiv \frac{1}{2}(m_u + m_d)$ is the average of the up and down current quark masses and σ_N is the nucleon σ term. The most recent estimate of the σ term is $\sigma_N \simeq 45\,\text{MeV}$, with an uncertainty of about 7–10 MeV [32]. We shall consider this uncertainty in Sec. IV.

The gluon condensate $\langle(\alpha_s/\pi)(\mathbf{E}^2 - \mathbf{B}^2)\rangle_{\rho_N}$ and the quark condensate $\langle\bar{q}iD_0 q\rangle_{\rho_N}$ are evaluated in Refs. [2,15] and Ref. [4], respectively:

$$\left\langle\frac{\alpha_s}{\pi}(\mathbf{E}^2 - \mathbf{B}^2)\right\rangle_{\rho_N} = -\frac{1}{2}\left\langle\frac{\alpha_s}{\pi}G^2\right\rangle_{\text{vac}} + (325\,\text{MeV})\rho_N , \tag{3.4}$$

$$\langle\bar{q}iD_0 q\rangle_{\rho_N} = \tfrac{3}{2}m_q\rho_N \simeq 0 . \tag{3.5}$$

The condensates $\langle(\alpha_s/\pi)(\mathbf{E}^2 + \mathbf{B}^2)\rangle_{\rho_N}$, $\langle q^\dagger iD_0 q\rangle_{\rho_N}$, and $\langle q^\dagger iD_0 iD_0 q\rangle_{\rho_N} + \frac{1}{12}\langle g_s q^\dagger\sigma\cdot\mathcal{G}q\rangle_{\rho_N}$ are estimated in Ref. [4] in terms of moments of parton distribution functions [33]. The results are

$$\left\langle\frac{\alpha_s}{\pi}(\mathbf{E}^2 + \mathbf{B}^2)\right\rangle_{\rho_N} = (100\,\text{MeV})\rho_N , \tag{3.6}$$

$$\langle q^\dagger iD_0 q\rangle_{\rho_N} = (180\,\mathrm{MeV})\rho_N \ , \qquad (3.7)$$

$$\langle q^\dagger iD_0 iD_0 q\rangle_{\rho_N} + \tfrac{1}{12}\langle g_s q^\dagger \sigma\cdot\mathcal{G}q\rangle_{\rho_N} = (176\,\mathrm{MeV})^2\rho_N \ . \tag{3.8}$$

To leading order in the nucleon density, the remaining condensates in the sum rules can be expanded as

$$\langle g_s q^\dagger \sigma\cdot\mathcal{G}q\rangle_{\rho_N} = \langle g_s q^\dagger \sigma\cdot\mathcal{G}q\rangle_N \rho_N + \cdots \ , \qquad (3.9)$$

$$\langle g_s\bar{q}\sigma\cdot\mathcal{G}q\rangle_{\rho_N} = \langle g_s\bar{q}\sigma\cdot\mathcal{G}q\rangle_{\mathrm{vac}} + \langle g_s\bar{q}\sigma\cdot\mathcal{G}q\rangle_N \rho_N + \cdots \ , \qquad (3.10)$$

$$\langle \bar{q}iD_0 iD_0 q\rangle_{\rho_N} + \tfrac{1}{8}\langle g_s\bar{q}\sigma\cdot\mathcal{G}q\rangle_{\rho_N}$$

$$= (\langle \bar{q}iD_0 iD_0 q\rangle_N + \tfrac{1}{8}\langle g_s\bar{q}\sigma\cdot\mathcal{G}q\rangle_N)\rho_N + \cdots \ . \tag{3.11}$$

The nucleon matrix element $\langle g_s q^\dagger \sigma\cdot\mathcal{G}q\rangle_N$ has been estimated previously in Refs. [34,35,4]. The range of the values from these estimates is $-0.33\,\mathrm{GeV}^2 \leq \langle g_s q^\dagger\sigma\cdot\mathcal{G}q\rangle_N \leq 0.66\,\mathrm{GeV}^2$; here we use $\langle g_s q^\dagger\sigma \cdot \mathcal{G}q\rangle_N = -0.33\,\mathrm{GeV}^2$, which is obtained from an analysis based on QCD sum rules [35]. In Ref. [4] simple bag-model estimates give $\langle g_s\bar{q}\sigma \cdot \mathcal{G}q\rangle_N \simeq 0.62\,\mathrm{GeV}^2$ and $\langle \bar{q}iD_0 iD_0 q\rangle_N + \tfrac{1}{8}\langle g_s\bar{q}\sigma \cdot \mathcal{G}q\rangle_{\rho_N} = 0.08\,\mathrm{GeV}^2$; other heuristic estimates lead to $\langle g_s\bar{q}\sigma \cdot \mathcal{G}q\rangle_N = 3\,\mathrm{GeV}^2$ and $\langle \bar{q}iD_0 iD_0 q\rangle_{\rho_N} + \tfrac{1}{8}\langle g_s\bar{q}\sigma \cdot \mathcal{G}q\rangle_{\rho_N} = 0.3\,\mathrm{GeV}^2$. We consider the latter values in this section. None of the three dimension-five condensates in Eqs. (3.9)–(3.11) have been determined accurately; the sensitivity of the sum-rule results to the precise values of these condensates will be given in Sec. IV.

Four-quark condensates are numerically important in both the vacuum and the finite-density nucleon sum rules because they contribute in tree diagrams and do not carry the numerical suppression factors typically associated with loops. In the sum rules derived in Sec. II, we included the contributions from the four-quark condensates in their in-medium factorized forms; however, the factorization approximation may not be justified in nuclear matter. In the case of the the "scalar-vector" and "vector-vector" four-quark condensates, $\langle\bar{q}q\rangle_{\rho_N}\langle q^\dagger q\rangle_{\rho_N}$ and $\langle q^\dagger q\rangle_{\rho_N}^2$, such concerns are unimportant, since these condensates give minimal contributions to the nucleon sum rules (see Sec. IV). Thus we use their factorized forms for simplicity. However, the "scalar-scalar" four-quark condensate $\langle\bar{q}q\rangle_{\rho_N}^2$ does give important contributions to the nucleon sum rules. In its factorized form, the scalar-scalar four-quark condensate has a very strong density dependence; one might suspect that this strong dependence is an artifact of the factorization approximation. Thus we choose to parametrize the scalar-scalar four-quark condensate so that it interpolates between its factorized form in free space and its factorized form in nuclear matter:

$$\langle\bar{q}q\rangle_{\rho_N}^2 \longrightarrow \langle\widetilde{\bar{q}q}\rangle_{\rho_N}^2 \equiv (1-f)\langle\bar{q}q\rangle_{\mathrm{vac}}^2 + f\langle\bar{q}q\rangle_{\rho_N}^2 \ , \qquad (3.12)$$

where f is a real parameter. The density dependence of the scalar-scalar four-quark condensate is thus parametrized by f and the density dependence of $\langle\bar{q}q\rangle_{\rho_N}$ [see Eq. (3.2)]. The factorized condensate $\langle\bar{q}q\rangle_{\rho_N}^2$ appearing in Eq. (2.31) will be replaced by $\langle\widetilde{\bar{q}q}\rangle_{\rho_N}^2$ in the calculations to follow. We consider values of f in the range of $0 \leq f \leq 1$; $f = 0$ corresponds to the assumption of no density dependence and $f = 1$ corresponds to the in-medium factorization assumption.

Several of the in-medium condensates are nonvanishing in the vacuum limit. The quark condensate $\langle\bar{q}q\rangle_{\mathrm{vac}}$ is related to the current quark mass through the Gell-Mann–Oakes–Renner relation

$$2m_q\langle\bar{q}q\rangle_{\mathrm{vac}} = -m_\pi^2 f_\pi^2 \ . \qquad (3.13)$$

The product $m_q\langle\bar{q}q\rangle_{\mathrm{vac}}$ is renormalization-group invariant, so fixing a value for the quark mass at the scale of interest fixes the value of the quark condensate in vacuum at the same scale. We take $m_\pi = 138\,\mathrm{MeV}$ and $f_\pi = 93\,\mathrm{MeV}$; in this section we take $\langle\bar{q}q\rangle_{\mathrm{vac}} \simeq -(245\,\mathrm{MeV})^3$ ($m_q \simeq 5.5\,\mathrm{MeV}$), which has been used in Ref. [3]. The sensitivity of our results to this choice will be tested in Sec. IV. We take $\langle(\alpha_s/\pi)G^2\rangle_{\mathrm{vac}} = (330\,\mathrm{MeV})^4$ [5,4] and $\langle g_s\bar{q}\sigma\cdot\mathcal{G}q\rangle_{\mathrm{vac}} = m_0^2\langle\bar{q}q\rangle_{\mathrm{vac}}$ with $m_0^2 = 0.8\,\mathrm{GeV}^2$ [7,4].

B. Sum-rule analysis

In principle, the predictions based on the sum rules in Sec. II should be independent of the auxiliary parameter M^2. In practice, however, we have to truncate the OPE and use a simple phenomenological *Ansatz* for the spectral density; thus one expects the two descriptions to overlap only in some limited range of M^2 (at best). As a result, one expects to see a "plateau" in the predicted quantities as functions of M^2. Studies of nucleon sum rules in vacuum truncated at dimension-six condensates do not provide a particularly convincing plateau [3,8,9]; nevertheless, we will assume that the sum rules actually have a region of overlap, although imperfect.[3] We follow Ref. [3] and rely on the cancellation of systematic discrepancies by normalizing finite-density predictions for all self-energies to the zero-density prediction for the mass. One hopes that this might compensate for general limitations of the sum rules. We fix the quasi-nucleon three-momentum at $|\mathbf{q}| = 270\,\mathrm{MeV}$; the dependence of the results on $|\mathbf{q}|$ will be presented in Sec. IV. All the finite-density results presented are obtained at nuclear matter saturation density, which is taken to be $\rho_N = (110\,\mathrm{MeV})^3$.

To analyze the sum rules and extract the self-energies, we sample the sum rules in the fiducial region, which is the overlap between the region where the sum rule is dominated by the quasinucleon contribution and the region where the truncated OPE is reliable. In choosing

---

[3]Including direct-instanton effects in nucleon sum rules in vacuum leads to a more convincing plateau [23,24].

the fiducial region, one may introduce a lower bound on the Borel mass such that the highest-dimensional condensates contribute no more than $\sim 10\%$ to the right-hand sides of Eqs. (2.30)–(2.32) and an upper bound on the Borel mass such that the continuum contributions are

less than $\sim 50\%$ of the total phenomenological contributions to the sum rules (i.e., the sum of the quasinucleon pole and the continuum contributions). To quantify the fit of the left- and right-hand sides, we use the logarithmic measure

$$\delta(M^2) = \ln\left[\frac{\max\{\lambda_N^{*2}e^{-(E_q^2-\mathbf{q}^2)/M^2}, \Pi_s'/M_N^*, \Pi_q', \Pi_u'/\Sigma_v\}}{\min\{\lambda_N^{*2}e^{-(E_q^2-\mathbf{q}^2)/M^2}, \Pi_s'/M_N^*, \Pi_q', \Pi_u'/\Sigma_v\}}\right] , \tag{3.14}$$

which is averaged over 150 points evenly spaced within the fiducial region of M^2. Here Π_s', Π_q', and Π_u' denote the right-hand sides of Eqs. (2.30)–(2.32), respectively. The predictions for M_N^*, Σ_v, s_0^*, and λ_N^{*2} are obtained by minimizing the averaged measure δ. This approach weights the fits in the region where the continuum contribution is minimal and reduces the sensitivity to the end points of the optimum region [9]. To get a prediction for the nucleon mass in vacuum, we apply the same procedure to the sum rules evaluated in the zero-density limit.

We first analyze the sum rules with the Borel window fixed at $0.8\,\text{GeV}^2 \le M^2 \le 1.4\,\text{GeV}^2$, which is identified by Ioffe and Smilga [8] as the fiducial region for the nucleon sum rules in vacuum (with contributions from condensates up to dimension nine included). Here we adopt these boundaries as the maximal limits of applicability of our sum rules at finite density. We start from Ioffe's interpolating field (i.e., $t = -1$), which has been used in earlier studies at finite density [1,3,4]. The optimized results for the ratios M_N^*/M_N, Σ_v/M_N, and E_q/M_N as functions of f are plotted in Fig. 1. (The two extreme cases, $f = 0$ and 1, have been studied in Ref. [3].) One can see from Fig. 1 that M_N^*/M_N and E_q/M_N vary rapidly with f while Σ_v/M_N is relatively insensitive to f. Therefore, the sum-rule prediction for the scalar self-energy depends *strongly* on the density dependence of the scalar-scalar four-quark condensate. For small values of f ($0 \le f \le 0.3$), the predictions are

$$M_N^*/M_N \simeq 0.63\text{–}0.72 , \tag{3.15}$$

$$\Sigma_v/M_N \simeq 0.24\text{–}0.30 , \tag{3.16}$$

which are comparable to typical values from relativistic phenomenology. On the other hand, for large f ($0.7 \le f \le 1.0$), we find $\Sigma_v/M_N \simeq 0.34$–0.37, which is still reasonable. In contrast, the predictions for M_N^* and E_q turn out to be $M_N^*/M_N \simeq 0.84$–0.94 and $E_q/M_N \simeq 1.24$–1.36, which implies $\Sigma_s/M_N \simeq 0.06$–0.16 and a significant shift in energy of the quasinucleon pole relative to the nucleon pole in vacuum (the net self-energy is repulsive). Thus a significant density dependence of the scalar-scalar four-quark condensate leads to an essentially vanishing scalar self-energy and a strong vector self-energy with a magnitude of a few hundred MeV. The predictions for the ratios $\lambda_N^{*2}/\lambda_N^2$ and s_0^*/s_0 also depend on f. For small f, the continuum threshold s_0^* is close to the vacuum value while the residue λ_N^{*2} drops about 20% relative to the corresponding vacuum value. (Note that these quantities are relatively poorly determined by the sum rules.) For large f, the continuum threshold increases by 20–25 % relative to the vacuum value and the residue at the pole increases by about 20%, implying a significant rearrangement of the spectrum. For intermediate values of f, both the continuum threshold and the residue are very close to the corresponding vacuum values.

From the sum rules in Eqs. (2.30)–(2.32), it is easy to see that the ratios Π_s'/Π_q' and Π_u'/Π_q' give M_N^* and Σ_v as functions of Borel M^2, and Π_s'/Π_q' in the zero-density limit yields M_N as a function of M^2. In Fig. 2, the ratios M_N^*/M_N and Σ_v/M_N are plotted as functions of M^2 for three different values of f, with E_q, $\overline{E}_q$ and the continuum threshold fixed at their optimized values. The curves for $f = 0$ and $f = 0.5$ (solid and dashed curves, respectively) are quite flat in the optimum region, and thus imply a weak dependence of the predicted ratios on M^2 (though the individual sum-rule predictions before taking ratios are not flat). For $f = 1$ (dotted curves), the ratio Σ_v/M_N is flat, indicating again a weak dependence on M^2; in contrast, M_N^*/M_N changes significantly in the region of interest.

To see how well the finite-density sum rules work, we plot $\lambda_N^{*2}e^{-(E_q^2-\mathbf{q}^2)/M^2}$, Π_s'/M_N^*, Π_q', and Π_u'/Σ_v as functions of M^2 for $f = 0$ in Fig. 3(a) using the predicted values for M_N^*, Σ_v, s_0^*, and λ_N^{*2}. If the sum rules work well, we should expect the four curves to coincide with each other. We find that their M^2 dependence in the Borel region of interest turns out to be equal up to 15%.
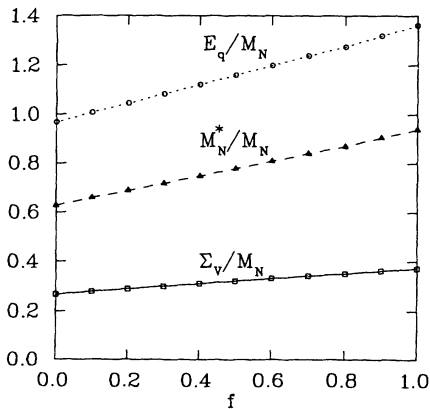
FIG. 1. Optimized sum-rule predictions for M_N^*/M_N, Σ_v/M_N, and E_q/M_N as functions of f, with Ioffe's interpolating field ($t = -1$). The other input parameters are described in the text.
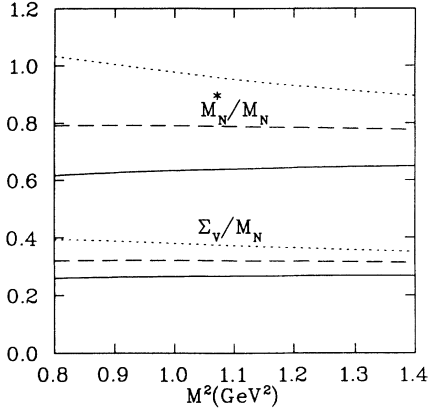
FIG. 2. Ratios M_N^*/M_N and Σ_v/M_N as functions of Borel M^2, with optimized predictions for E_q, $\overline{E}_q$ and the continuum threshold. The solid, dashed, and dotted curves correspond to $f = 0$, 0.5, and 1.0, respectively. The other parameters are the same as in Fig. 1.
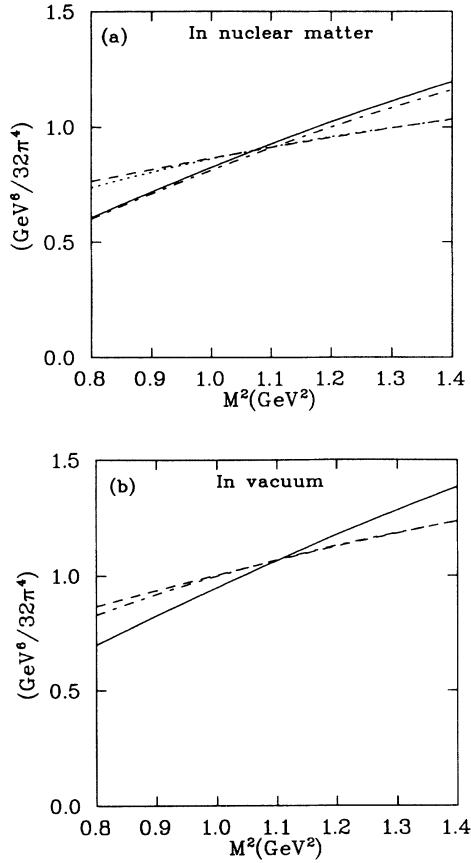
FIG. 3. (a) The left- and right-hand sides of the finite-density sum rules as functions of Borel M^2 for $t = -1$ and $f = 0$, with the optimized values for M_N^*, Σ_v, s_0^*, and λ_N^{*2}. The other parameters are the same as in Fig. 1. The four curves correspond to Π_s'/M_N^* (solid), Π_q' (dashed), Π_u'/Σ_v (dot-dashed), and $\lambda_N^{*2}e^{-(E_q^2-q^2)/M^2}$ (dotted). (b) The left- and right-hand sides of the corresponding vacuum sum rules. The three curves correspond to Π_s'/M_N (solid), Π_q' (dashed), and $\lambda_N^2 e^{-M_N^2/M^2}$ (dot-dashed) at the zero-density limit, with the optimized values for M_N, s_0, and λ_N^2.

The overlap of the corresponding vacuum sum rules (i.e., the zero-density limit) is illustrated in Fig. 3(b). We observe that the quality of the overlap for the finite-density sum rules is similar to that of the corresponding sum rules in vacuum, and as f increases, the overlap of the sum rules gets better.

All of the results above use Ioffe's interpolating field ($t = -1$); we now present the results for the general interpolating field [Eq. (2.4)]. In Fig. 4 we have displayed the predicted ratios M_N^*/M_N and Σ_v/M_N as functions of t for three different values of f. The ratio Σ_v/M_N increases as t increases (over the range of t considered); the rate of increase is essentially the same for all values of f. For $f = 1$, the ratio M_N^*/M_N decreases slowly as t increases; for $f = 0.5$, M_N^*/M_N is nearly independent of t; for $f = 0.2$, M_N^*/M_N increases slowly as t increases. We find that the continuum contributions increase and the residue decreases as t increases. On the other hand, the overlap of the sum rules gets better as t increases. The prediction for the continuum threshold depends only weakly on t. We also find that for $f < 0.2$ and $-1.15 \leq t \leq -1.05$, the numerical optimizing procedure converges slowly and the predicted continuum threshold and residue are much smaller than those for $f \geq 0.2$. In this case, the continuum contributions dominate the sum rules making the predictions for M_N^* and Σ_v unreliable.

We proceed now to analyze the sum rules by taking an upper bound of the Borel window such that the continuum contributions to the phenomenological sides do not exceed 50%, while fixing the lower bound at $0.8\,\text{GeV}^2$. The lower bound is fixed since we have not included contributions from dimension-seven and higher-dimensional condensates. Studies of nucleon sum rules in vacuum [8,9,3] suggest that contributions from these higher-dimensional condensates are small for $M^2 \geq 0.8\,\text{GeV}^2$; thus we expect that the lower bound at $0.8\,\text{GeV}^2$ is reasonable for nucleon sum rules at finite density. The two solid lines in Fig. 5 are the predicted values of M_N^*/M_N and Σ_v/M_N for $f = 0.5$ obtained by choosing the Borel window (at each t) such that the continuum contributions are less than 50% (at the upper bound). We have used the same procedure in extracting the nucleon mass
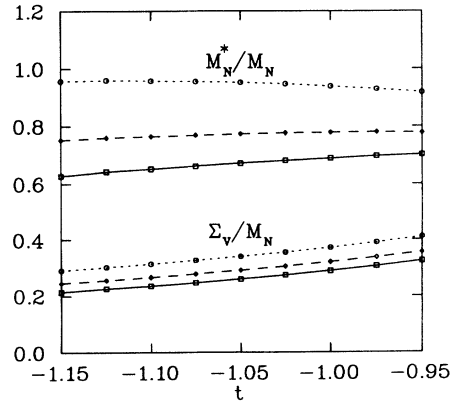
FIG. 4. Optimized sum-rule predictions for M_N^*/M_N and Σ_v/M_N as functions of t. The three curves correspond to $f = 0.2$ (solid), 0.5 (dashed), and 1.0 (dotted).
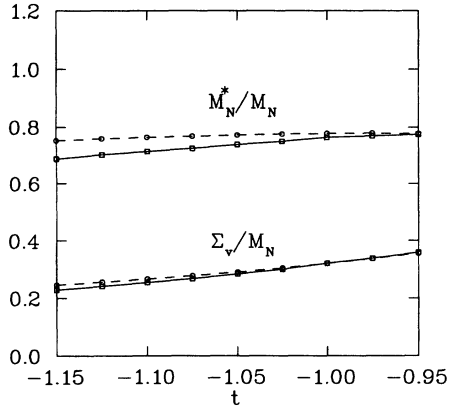
FIG. 5. Optimized sum-rule predictions for M_N^*/M_N and Σ_v/M_N as functions of t, with $f = 0.5$. The solid curves correspond to the results obtained by requiring the continuum contributions to be less than 50% in the fiducial Borel region and the dashed curves correspond to the results obtained using a fixed Borel window at $0.8\,\text{GeV}^2 \leq M^2 \leq 1.4\,\text{GeV}^2$.

in vacuum. The two dashed curves in Fig. 5 correspond to M_N^*/M_N and Σ_v/M_N obtained using a fixed Borel window at $0.8\,\text{GeV}^2 \leq M^2 \leq 1.4\,\text{GeV}^2$, with the same inputs. We see that the two curves for Σ_v/M_N overlap, implying that changing the upper limit of the optimum Borel region does not affect the sum-rule prediction for the ratio Σ_v/M_N. For M_N^*/M_N, the discrepancy between the two curves is about 5–10 % at lower values of t; this discrepancy eventually disappears as t increases. Thus our results for the two ratios are quite stable and nearly unaffected by the choice of the upper bound of the Borel window. The predicted continuum threshold and residue depend weakly on the upper limit of the fiducial region. We also find that the resulting Borel window shrinks as t increases.

We have seen the important role of the scalar-scalar four-quark condensate in determining the scalar self-energy and the dependence of the predictions on the choice of the nucleon interpolating field. To see the effects of the other condensates and parameters, we shall test the sensitivity of our results to changes in these condensates and parameters.

IV. SENSITIVITY ANALYSIS

In this section we first present the three-momentum dependence of the predictions and test the stability of the predictions to the choice of $\overline{E}_q$. We then examine the sensitivity and stability of the extracted ratios M_N^*/M_N and Σ_v/M_N to individual condensates and parameters. When we change a particular condensate or parameter, the rest are held fixed at the values given in Sec. III. We also give an estimate of the overall sensitivity of the predictions to all of the dimension-five condensates. We use a fixed Borel window, $0.8\,\text{GeV}^2 \leq M^2 \leq 1.4\,\text{GeV}^2$, and choose $t = -1$.

We start with the three-momentum $|\mathbf{q}|$ dependence of the sum-rule predictions. In our finite-density sum-

rule approach, $|\mathbf{q}|$ labels *distinct* quasiparticle states with different self-energies. The three-momentum enters the sum rules only through $\overline{E}_q$, the combination $\overline{E}_q^2 - \mathbf{q}^2$, and in factors of $\mathbf{q}^2$ that accompany some of the higher-dimensional condensates. The three-momentum dependence of the predicted ratios is illustrated in Fig. 6. The result for Σ_v/M_N is nearly independent of $|\mathbf{q}|$ for $|\mathbf{q}| \leq 1.0\,\text{GeV}$; the result for M_N^*/M_N depends only weakly on $|\mathbf{q}|$ for $|\mathbf{q}| \leq 0.5\,\text{GeV}$. This, if interpreted in terms of relativistic nuclear phenomenology, implies that the real parts of the scalar and vector optical potentials seen by a scattered nucleon are weakly dependent on energy. While the ratio M_N^*/M_N changes significantly over the range $0.5\,\text{GeV} < |\mathbf{q}| \leq 1.0\,\text{GeV}$, we do not expect that a sharp quasiparticle *Ansatz* is reasonable at such high momenta [13].

As noted in Sec. II, the positive-energy quasinucleon pole assumption and Lorentz covariance lead to the introduction of a negative-energy quasinucleon pole at $\overline{E}_q = \Sigma_v - \sqrt{\mathbf{q}^2 + M_N^{*2}}$. To suppress contributions to the sum rules from negative-energy excitations and focus only on the positive-energy quasinucleon state, we apply a transformation that depends explicitly on $\overline{E}_q$ [see Eq. (2.27)]. This transformation eliminates the contribution from a sharp negative-energy pole at $\overline{E}_q$ and strongly suppresses a broad excitation in the vicinity of $\overline{E}_q$. Thus, for the present approach to be reliable, we should find that the extracted quasinucleon self-energies are fairly insensitive to the precise value of $\overline{E}_q$; to test this, we *assign* a value to $\overline{E}_q$ in the sum rules. The resulting Σ_v and M_N^* do *not*, in general, satisfy the pole constraint of Eq. (2.13). In Fig. 7 the predictions for M_N^*/M_N and Σ_v/M_N are plotted as functions of $\overline{E}_q$ over the region $-0.7\,\text{GeV} \leq \overline{E}_q \leq -0.3\,\text{GeV}$ for three values of f. The values of $\overline{E}_q$ that satisfy Eq. (2.13) are $-0.38\,\text{GeV}$, $-0.45\,\text{GeV}$, and $-0.53\,\text{GeV}$ for $f = 0$, 0.5, and 1.0, respectively. We see that M_N^*/M_N is fairly insensitive to $\overline{E}_q$, and Σ_v/M_N varies less than 15% in the given region. This indicates that the predictions are reasonably stable.
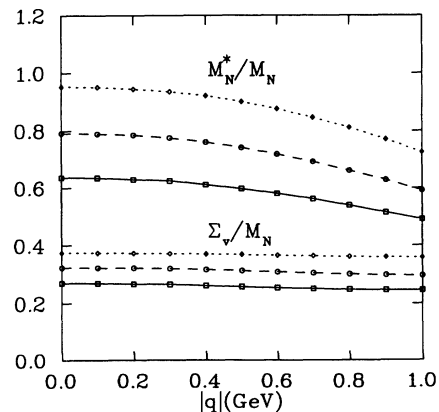
FIG. 6. Three-momentum dependence of the predicted M_N^*/M_N and Σ_v/M_N, with $t = -1$. The three curves correspond to $f = 0$ (solid), 0.5 (dashed), and 1.0 (dotted). The other parameters are the same as in Fig. 1.
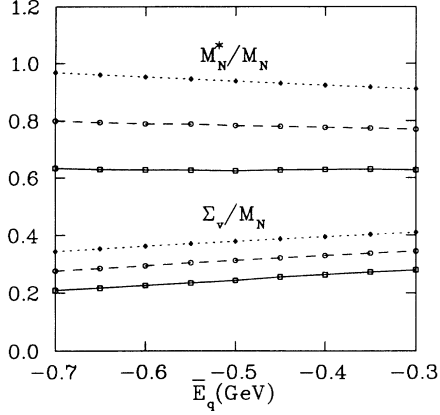
FIG. 7. Optimized sum-rule predictions for M_N^*/M_N and Σ_v/M_N as functions of $\overline{E}_q$, with $t = -1$. The three curves correspond to $f = 0$ (solid), 0.5 (dashed), and 1.0 (dotted). The other parameters are the same as in Fig. 1.

We now turn to study the sensitivity of the sum-rule predictions to the condensates and other input parameters. The vacuum quark condensate $\langle \overline{q}q \rangle_{\rm vac}$ appears implicitly in the finite-density sum rules through the in-medium quark condensate $\langle \overline{q}q \rangle_{\rho_N}$, which appears at leading order of the OPE [see Eq. (2.30)], and the factorized four-quark condensates. Here we consider the range $\langle \overline{q}q \rangle_{\rm vac} \simeq -(225\text{-}250\,\text{MeV})^3$ $(m_q \simeq 5\text{-}7\,\text{MeV})$, which includes the typical values used in QCD sum-rule applications. With a smaller value for $\langle \overline{q}q \rangle_{\rm vac}$, the contributions from higher-order terms in the OPE become more important relative to the leading-order term, and the predicted nucleon mass at zero density becomes smaller. In Fig. 8 we present M_N^*/M_N and Σ_v/M_N as functions of $\langle \overline{q}q \rangle_{\rm vac}^{1/3}$. The ratio M_N^*/M_N is insensitive to the vacuum quark condensate; on the other hand, the ratio Σ_v/M_N changes significantly within the interval considered. We note that the nucleon mass increases and Σ_v decreases as the magnitude of the vacuum quark condensate increases; this leads to a large variation of Σ_v/M_N with $\langle \overline{q}q \rangle_{\rm vac}$.
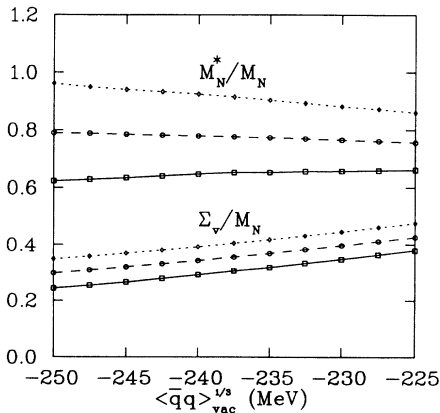
The nucleon σ term σ_N also enters the sum rules through the in-medium quark condensate $\langle \overline{q}q \rangle_{\rho_N}$ and the four-quark condensates. It also affects the in-medium gluon condensate [2]. However, this effect is tiny in the range of σ_N that is of interest; we ignore the change in the in-medium gluon condensate when we vary σ_N. In Fig. 9 we plot M_N^*/M_N and Σ_v/M_N as functions of σ_N for the range $35\,\text{MeV} \leq \sigma_N \leq 55\,\text{MeV}$, which covers the uncertainty given in Ref. [32]. The prediction for Σ_v/M_N is fairly insensitive to σ_N. In contrast, M_N^*/M_N changes significantly and varies by about 15% in the given region, which implies a factor of 2 variation in the scalar self-energy. This reflects the important role of the terms involving $\langle \overline{q}q \rangle_{\rho_N}$ in determining the scalar self-energy. At the upper bound $\sigma_N = 55\,\text{MeV}$, the scalar self-energy appears to be large for $f \leq 0.5$. (For $f < 0.1$ and $52\,\text{MeV} < \sigma_N \leq 55\,\text{MeV}$, one cannot find reliable predictions.)

The sensitivity of the predictions to the nucleon matrix element $\langle g_s q^\dagger \sigma \cdot \mathcal{G} q \rangle_N$ is shown in Fig. 10. We have fixed $\langle q^\dagger i D_0 i D_0 q \rangle_N + \frac{1}{12} \langle g_s q^\dagger \sigma \cdot \mathcal{G} q \rangle_N$ at the value given in Eq. (3.8), since this combination can be determined reliably in terms of parton distribution functions. The prediction for M_N^*/M_N is insensitive to $\langle g_s q^\dagger \sigma \cdot \mathcal{G} q \rangle_N$. On the other hand, the ratio Σ_v/M_N varies by about 20% in the given region. This variation indicates that the fourth term on the right-hand side of Eq. (2.32) may contribute up to 20% of Π_u. For $f < 0.2$ and $0.7\,\text{GeV}^2 < \langle g_s q^\dagger \sigma \cdot \mathcal{G} q \rangle_N \leq 1.0\,\text{GeV}^2$, we do not find any reliable predictions.

The sensitivity of the sum-rule results to the nucleon matrix element $\langle \overline{q} i D_0 i D_0 q \rangle_N + \frac{1}{8} \langle g_s \overline{q} \sigma \cdot \mathcal{G} q \rangle_N$ is plotted in Fig. 11. The predictions for M_N^*/M_N and Σ_v/M_N are insensitive to the precise value of this matrix element, implying that the contributions from the corresponding condensate are small relative to those of the leading-order terms. We do not consider independent variations in the condensate $\langle g_s \overline{q} \sigma \cdot \mathcal{G} q \rangle_{\rho_N}$, which only appears on the right-hand side of Eq. (2.30) multiplied by $c_2 = 1 - t^2$, which vanishes for $t = -1$. For other values of t of interest

FIG. 8. Optimized sum-rule predictions for M_N^*/M_N and Σ_v/M_N as functions of $\langle \overline{q}q \rangle_{\rm vac}^{1/3}$. The three curves correspond to $f = 0$ (solid), 0.5 (dashed), and 1.0 (dotted). The other parameters are the same as in Fig. 1.
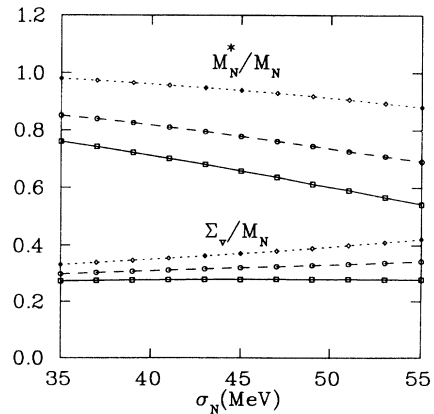
FIG. 9. Optimized sum-rule predictions for M_N^*/M_N and Σ_v/M_N as functions of the nucleon σ term σ_N, with $t = -1$. The three curves correspond to $f = 0.1$ (solid), 0.5 (dashed), and 1.0 (dotted). The other parameters are the same as in Fig. 1.
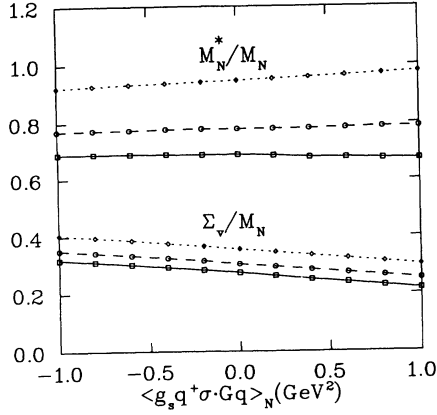
FIG. 10. Optimized sum-rule predictions for M_N^*/M_N and Σ_v/M_N as functions of the nucleon matrix element $\langle g_s q^\dagger \sigma \cdot \mathcal{G}q \rangle_N$, with $t = -1$. The three curves correspond to $f = 0.2$ (solid), 0.5 (dashed), and 1.0 (dotted). The other parameters are the same as in Fig. 1.
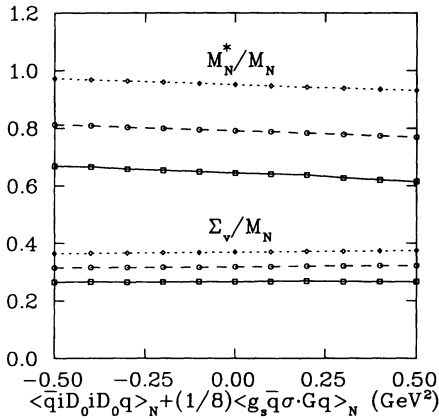
FIG. 11. Optimized sum-rule predictions for M_N^*/M_N and Σ_v/M_N as functions of the nucleon matrix element $\langle \bar{q}iD_0iD_0q \rangle_N + \frac{1}{8}\langle g_s \bar{q}\sigma \cdot \mathcal{G}q \rangle_N$, with $t = -1$. The three curves correspond to $f = 0$ (solid), 0.5 (dashed), and 1.0 (dotted). The other parameters are the same as in Fig. 1.
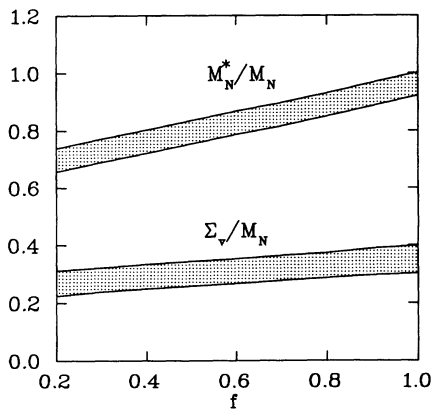
FIG. 12. Optimized sum-rule predictions for M_N^*/M_N and Σ_v/M_N as functions of f, with $t = -1$. The shaded areas represent the uncertainties due to the variations of all the dimension-five condensates in their range of values given in the text.

TABLE I. The changes in the predicted ratios M_N^*/M_N and Σ_v/M_N when the individual condensates are changed by $\pm 20\%$ relative to their values given in Sec. III and Λ_{QCD} is changed from 100 MeV to 200 MeV, with fixed $t = -1$ and $f = 0.5$.

Condensates and parameters	M_N^*/M_N	Σ_v/M_N
$\langle q^\dagger iD_0 q \rangle_{\rho_N} \pm 20\%$	0%	$\mp 7\%$
$\langle (\alpha_s/\pi)(\mathbf{E}^2 - \mathbf{B}^2) \rangle_{\rho_N} \pm 20\%$	$\mp 2\%$	$\mp 2\%$
$\langle (\alpha_s/\pi)(\mathbf{E}^2 + \mathbf{B}^2) \rangle_{\rho_N} \pm 20\%$	0%	0%
$\langle q^\dagger iD_0 iD_0 q \rangle_{\rho_N} + \frac{1}{12}\langle g_s q^\dagger \sigma \cdot \mathcal{G}q \rangle_{\rho_N} \pm 20\%$	0%	0%
$\langle \bar{q}q \rangle_{\rho_N} \langle q^\dagger q \rangle_{\rho_N} \pm 20\%$	$\mp 1\%$	0%
$\langle q^\dagger q \rangle_{\rho_N}^2 \pm 20\%$	0%	0%
$\Lambda_{QCD}(100 \rightarrow 200\,\text{MeV})$	$+2\%$	-9%

here, c_2 is small and we expect that the predictions are insensitive to the precise value of $\langle g_s \bar{q}\sigma \cdot \mathcal{G}q \rangle_{\rho_N}$.

To test the sensitivity to the remaining condensates and parameters, we change individual condensates by $\pm 20\%$ relative to their values given in Sec. III and change Λ_{QCD} from 100 MeV to 200 MeV. The results for the changes in the predicted ratios are given in Table I. One can see that the changes in most of the listed condensates cause only tiny changes in the predictions, showing that the contributions from these condensates to the sum rules are very small. The changes in $\langle q^\dagger iD_0 q \rangle_{\rho_N}$ and Λ_{QCD} lead to changes that are small but not completely negligible.

Finally, we test the overall sensitivity of the predicted ratios to all of the dimension-five condensates appearing in the OPE. Since these condensates are not well determined, we consider the ranges

$$-1\,\text{GeV}^2 \leq \langle g_s q^\dagger \sigma \cdot \mathcal{G}q \rangle_N \leq 1\,\text{GeV}^2 , \qquad (4.1)$$

$$-0.5\,\text{GeV}^2 \leq \langle \bar{q}iD_0 iD_0 q \rangle_N + \frac{1}{8}\langle g_s \bar{q}\sigma \cdot \mathcal{G}q \rangle_N \leq 0.5\,\text{GeV}^2 , \qquad (4.2)$$

and vary the condensate $\langle q^\dagger iD_0 iD_0 q \rangle_{\rho_N} + \frac{1}{12}\langle g_s q^\dagger \sigma \cdot \mathcal{G}q \rangle_{\rho_N}$ by $\pm 20\%$ relative to the value used in Sec. III. All remaining condensates are held fixed at the values given in Sec. III. We then randomly choose 200 points in the *combined* range of these condensates. The resulting maximum and minimum of M_N^*/M_N and Σ_v/M_N determine the overall uncertainty. The results are presented in Fig. 12, where the shaded areas reflect the combined variations of the dimension-five condensates in the above ranges. For $f < 0.2$, reliable predictions cannot be obtained in some of the randomly chosen points (in particular the points with $\langle g_s q^\dagger \sigma \cdot \mathcal{G}q \rangle_N$ large and positive).

V. DISCUSSION

The most important and concrete conclusion we can draw from this work is that QCD sum rules predict a positive vector self-energy with a magnitude of a few hundred MeV for a quasinucleon in nuclear matter. This qualitative feature is, for the most part, independent of the details of the calculation and is stable against variations of the condensates and the choice of interpolating

field. For Ioffe's interpolating field and typical values of the relevant condensates and other input parameters, one obtains $\Sigma_v/M_N \simeq 0.24$–0.37, which is a range very similar to that found for vector self-energies in relativistic nuclear physics phenomenology. On the other hand, the prediction for the scalar self-energy depends strongly on the value of the in-medium scalar-scalar four-quark condensate, which is not well established, and on the value of the nucleon σ term. This means that our conclusions about the quasinucleon scalar self-energy must still be somewhat indefinite. Nevertheless, we emphasize that the predictions with different values of the scalar-scalar four-quark condensate give different physical features that are not equally compatible with known nuclear phenomenology.

If the four-quark condensates depend only weakly on the nucleon density (i.e., if f is small), we find that the prediction for M_N^*/M_N is insensitive to the Borel mass. The predicted scalar self-energy is large and negative, which is consistent with relativistic phenomenology. In this case, there is a significant degree of cancellation between the scalar and vector self-energies. This feature leads to a quasinucleon energy close to the free-space nucleon mass. This result is compatible with the empirical observation that the quasinucleon energy is shifted only slightly in nuclear matter relative to the free-space mass. The prediction for the continuum threshold is close to the vacuum value and the residue at the quasinucleon pole drops slightly relative to the corresponding vacuum value. This is also compatible with experiment; there is no evidence for a strong rearrangement of the spectrum at nuclear matter saturation density, merely a spreading of strength over energy scales too small to be resolved by the sum rules.

In contrast, if the four-quark condensates have a strong density dependence (i.e., if f is large), the predicted ratio M_N^*/M_N varies strongly with the Borel mass, and the magnitude of M_N^*/M_N is close to unity, implying that the scalar self-energy is essentially zero. The predicted vector self-energy, on the other hand, is larger than it is with small f. Thus the resulting quasinucleon energy is significantly larger than the nucleon mass. This result is unrealistic and is totally different from known nuclear phenomenology. Moreover, both the continuum threshold and the residue at the quasinucleon pole are well above their values in vacuum; this suggests a significant rearrangement of the spectrum in nuclear matter, which is inconsistent with experiment.

For intermediate values of f, the predicted scalar self-energy is negative with a sizable magnitude. The vector self-energy is still strong. The magnitudes of the self-energies and the degree of cancellation between them depend on the choice of interpolating field and the values of the condensates and input parameters. The quasinucleon energy, the residue at the quasinucleon pole, and the continuum threshold are close to their corresponding vacuum values.

The qualitative features discussed above can also be identified through the dominant behavior of the OPE sides of the sum rules. From Eq. (2.31), we note that Π_q' is mainly determined by the density-independent leading-order perturbative term and the scalar-scalar four-quark condensate. For small f, Π_q' is close to its zero-density value; this implies that the quasinucleon energy, residue, and continuum are essentially unchanged from their values in vacuum. Since Π_s' is dominated by the leading-order term proportional to the in-medium quark condensate, the significant reduction of $\langle \bar{q}q \rangle_{\rho_N}$ from its vacuum value $\langle \bar{q}q \rangle_{\rm vac}$ implies a significant reduction of M_N^* from M_N. The vector self-energy simply follows the nucleon density, as the leading-order term proportional to $\langle q^\dagger q \rangle_{\rho_N}$ gives the largest contribution to Π_u'. For large values of f, Π_q' is significantly reduced from its vacuum value; this leads to a shift in the quasinucleon energy and a significant rearrangement of the spectrum. As Π_s' and Π_u' are independent of f, one expects M_N^* and Σ_v to increase due to the reduction of Π_q'. Clearly, further study of the in-medium four-quark condensates is very important.

The sum-rule predictions are fairly sensitive to the choice of interpolating field, reflecting the dependence of the truncated OPE on this choice (see Figs. 4 and 5). In the region $-1.15 \leq t \leq -1$, we see that the scalar and vector self-energies (recall $\Sigma_s = M_N^* - M_N$) each have a magnitude of a few hundred MeV with opposite signs for $f < 0.5$, which is in qualitative agreement with relativistic phenomenology. As t gets larger, smaller f values are needed to produce large and canceling scalar and vector self-energies. In the interval of t considered here, the contributions of higher-order terms in the OPE become more important for larger magnitudes of t. For smaller magnitudes of t, the continuum contributions become larger, and the coupling of the interpolating field to the quasinucleon states becomes weaker. Since there is less information about the higher-dimensional condensates and we are only interested in the quasinucleon state, one should not use t with a magnitude that is too large or too small. Within the range of t considered in the present work, the vector self-energy is always large; the scalar self-energy is mainly controlled by the value of f.

The nucleon σ term σ_N is a crucial phenomenological input in the finite-density nucleon sum rules (see Fig. 9); its value determines the degree of chiral restoration in the nuclear medium (to first order in the nucleon density). As noted previously [1,3], the scalar self-energy strongly depends on σ_N through $\langle \bar{q}q \rangle_{\rho_N}$ and the four-quark condensates. We observe that the large and canceling self-energies found with small and moderate f values mainly depend on the ratio σ_N/m_q [1,3]. How do we understand this? This subject is under active investigation [36]. An understanding of the cancellation between scalar and vector components will be essential in making connections between QCD and nuclear physics.

Even if we assume that the scalar-scalar four-quark condensate has weak or moderate density dependence (so that the sum-rule predictions are consistent with known relativistic phenomenology), there are still some important open questions to confront. The large and canceling scalar and vector self-energies found in the nucleon case may not be predicted for other baryons, leading to possible contradictions with experiment. We must test sum rules for other baryons as well as for other nucleon properties. The Δ and the Λ should be particularly informa-

tive. There is useful information on the Δ in the nuclear medium from both electron and proton scattering from nuclei. Since the Δ sum rule is especially sensitive to the scalar-scalar four-quark condensate [6,9], we may obtain some additional phenomenological constraints on its density dependence. Work in this direction is in progress.

ACKNOWLEDGMENTS

[1] T. D. Cohen, R. J. Furnstahl, and D. K. Griegel, Phys. Rev. Lett. 67, 961 (1991).

[2] T. D. Cohen, R. J. Furnstahl, and D. K. Griegel, Phys. Rev. C 45, 1881 (1992).

[3] R. J. Furnstahl, D. K. Griegel, and T. D. Cohen, Phys. Rev. C 46, 1507 (1992).

[4] X. Jin, T. D. Cohen, R. J. Furnstahl, and D. K. Griegel, Phys. Rev. C 47, 2882 (1993).

[5] M. A. Shifman, A. I. Vainshtein, and V. I. Zakharov, Nucl. Phys. B147, 385 (1979); B147, 448 (1979); B147, 519 (1979).

[6] B. L. Ioffe, Nucl. Phys. B188, 317 (1981); B191, 591(E) (1981).

[7] V. M. Belyaev and B. L. Ioffe, Zh. Eksp. Teor. Fiz. 83, 876 (1982) [Sov. Phys. JETP 56, 493 (1982)]; 84, 1236 (1983) [57, 716 (1983)].

[8] B. L. Ioffe and A. V. Smilga, Nucl. Phys. B232, 109 (1984).

[9] D. B. Leinweber, Ann. Phys. (N.Y.) 198, 203 (1990).

[10] For a review, see L. J. Reinders, H. Rubinstein, and S. Yazaki, Phys. Rep. 127, 1 (1985), and references therein.

[11] B. D. Serot and J. D. Walecka, Adv. Nucl. Phys. 16, 1 (1986); B. D. Serot, Rep. Prog. Phys. 55, 1855 (1992).

[12] F. de Jong and R. Malfliet, Phys. Rev. C 44, 998 (1991).

[13] S. J. Wallace, Annu. Rev. Nucl. Part. Sci. 37, 267 (1987).

[14] S. Hama, B. C. Clark, E. D. Cooper, H. S. Sherif, and R. L. Mercer, Phys. Rev. C 41, 2737 (1990).

[15] E. G. Drukarev and E. M. Levin, Pis'ma Zh. Eksp. Teor. Fiz. 48, 307 (1988) [JETP Lett. 48, 338 (1988)]; Zh. Eksp. Teor. Fiz. 95, 1178 (1989) [Sov. Phys. JETP 68, 680 (1989)]; Nucl. Phys. A511, 679 (1990); A516, 715(E) (1990); Prog. Part. Nucl. Phys. 27, 77 (1991).

[16] E. M. Henley and J. Pasupathy, Nucl. Phys. A556, 467 (1993).

[17] T. Hatsuda, H. Høgaasen, and M. Prakash, Phys. Rev. Lett. 66, 2851 (1991).

[18] C. Adami and G. E. Brown, Z. Phys. A 340, 93 (1991).

[19] T. Hatsuda and S. H. Lee, Phys. Rev. C 46, R34 (1992).

[20] M. Asakawa and C. M. Ko, Nucl. Phys. A560, 399 (1993); Phys. Rev. C 48, R526 (1993).

[21] B. L. Ioffe, Z. Phys. C 18, 67 (1983).

[22] D. Espriu, P. Pascual, and R. Tarrach, Nucl. Phys. B214, 285 (1983).

[23] A. E. Dorokhov and N. I. Kochelev, Z. Phys. C 46, 281 (1990).

[24] H. Forkel and M. K. Banerjee, Phys. Rev. Lett. 71, 484 (1993).

[25] M. Sugawara and A. Kanazawa, Phys. Rev. 123, 1895 (1961).

[26] K. G. Wilson, Phys. Rev. 179, 1499 (1969).

[27] J. C. Collins, Renormalization (Cambridge University Press, New York, 1984).

[28] A. I. Vainshtein, V. I. Zakharov, V. A. Novikov, and M. A. Shifman, Yad. Fiz. 41, 1063 (1985) [Sov. J. Nucl. Phys. 41, 683 (1985)], and references therein; V. A. Novikov, M. A. Shifman, A. I. Vainshtein, and V. I. Zakharov, Nucl. Phys. B249, 445 (1985), and references therein.

[29] F. David, Nucl. Phys. B263, 637 (1986), and references therein.

[30] M. E. Peskin, Phys. Lett. 88B, 128 (1979).

[31] R. J. Furnstahl, Ohio State University Report No. OSU-0901 (1993).

[32] J. Gasser, H. Leutwyler, and M. E. Sainio, Phys. Lett. B 253, 252 (1991).

[33] M. Glück, E. Reya, and A. Vogt, Z. Phys. C 48, 471 (1990); 53, 127 (1992).

[34] E. V. Shuryak and A. I. Vainshtein, Phys. Lett. 105B, 65 (1981); Nucl. Phys. B199, 451 (1982).

[35] V. M. Braun and A. V. Kolesnichenko, Nucl. Phys. B283, 723 (1987).

[36] X. Jin, M. Nielsen, and J. Pasupathy, Phys. Lett. B 314, 163 (1993).

FIG. 12. Optimized sum-rule predictions for M_N^*/M_N and Σ_v/M_N as functions of f, with $t = -1$. The shaded areas represent the uncertainties due to the variations of all the dimension-five condensates in their range of values given in the text.